Metrologia **45** (2008) S59–S65 doi:10.1088/0026-1394/45/6/S10

Progress in the generation of the UTC(CNM) in terms of a virtual clock

J M López-Romero and N Díaz-Muñoz

Time and Frequency Division, Centro Nacional de Metrología, CENAM, km 4.5 carretera a los Cues, El Marqués, 76241, Querétaro, Mexico

E-mail: mauricio.lopez@cenam.mx

Received 15 July 2008, in final form 23 October 2008
Published 5 December 2008
Online at stacks.iop.org/Met/45/S59

Abstract

The Time and Frequency Division of the Centro Nacional de Metrología (CENAM) has developed and implemented a time scale algorithm in order to give better characteristics of stability, accuracy and robustness to the UTC(CNM). The UTC(CNM) has been generated since March 1996 with no interruptions and since MJD 53 000 the |UTC − UTC(CNM)| time differences were smaller than 50 ns during more than 90% of the time. When time differences were bigger than 50 ns they were smaller than 80 ns; time stability of the UTC(CNM) was 4.3 ns for 5 days and 30 ns for 1 year. With the new method to generate the UTC(CNM), time differences |UTC − UTC(CNM)| no bigger than 25 ns, a time stability of 2 ns for 5 days and 15 ns for 1 year are expected. In this paper we report on the progress made at the CENAM Time and Frequency Division to generate the UTC(CNM) in terms of a virtual clock. We present and discuss preliminary results when the time scale algorithm is implemented on four industrial Cs clocks (two of them high performance clocks) and one active hydrogen maser.

(Some figures in this article are in colour only in the electronic version)

1. Introduction

A group of clocks, also called an ensemble, can be used to generate a time scale with superior metrological characteristics to those obtainable from any single clock member of the ensemble. Time keeping for critical applications, such as the generation of the UTC(k) time scales, requires very high characteristics on reliability, stability and accuracy. Because of the susceptibility to failure of any single clock, national measurement institutes (NMIs) usually keep working more than one clock in order to generate its own prediction of the UTC, called UTC(k), where k is an acronym for the NMI, with high reliability. The most efficient use of such an ensemble of clocks implies the generation of a time scale, also called the averaged time scale, based on the operation of the set of clocks. The Coordinated Universal Time scale of the Centro Nacional de Metrología (CENAM), UTC(CNM), has been generated since MJD 50 143 (March 1996) [1] with no interruptions and since MJD 53 000 the |UTC − UTC(CNM)| time differences have been smaller than 50 ns during more than 90% of the time. When these time differences were bigger than 50 ns they were also smaller than 80 ns (see figure 1). During the time interval from MJD 53 000 to MJD 54 554 the time stability of the UTC(CNM) was 4.3 ns for 5 days and 30 ns for 1 year. Since MJD 50 143 the UTC(CNM) has been generated by the 1 pps output of a single Cs high performance clock from a set of at least four Cs clocks, referred to as the Master Clock. More recently, the CENAM Time and Frequency Division has developed and implemented a time scale algorithm in order to make efficient use of its ensemble of atomic clocks and then improve the UTC(CNM) characteristics of stability, accuracy, reliability and robustness. In this paper we report on the progress made at the CENAM to generate the UTC(CNM) in terms of such an averaged time scale.

We present and discuss the time scale algorithm used at the CENAM Time and Frequency Division as well as its implementation. Preliminary results obtained by using four commercial Cs clocks and one active hydrogen maser are also discussed. Much of the basic analysis presented in section 2 is presented in detail elsewhere [2–4], but is summarized here for completeness. Section 3 is devoted to present measurements on the time scale. In section 4 we discuss the

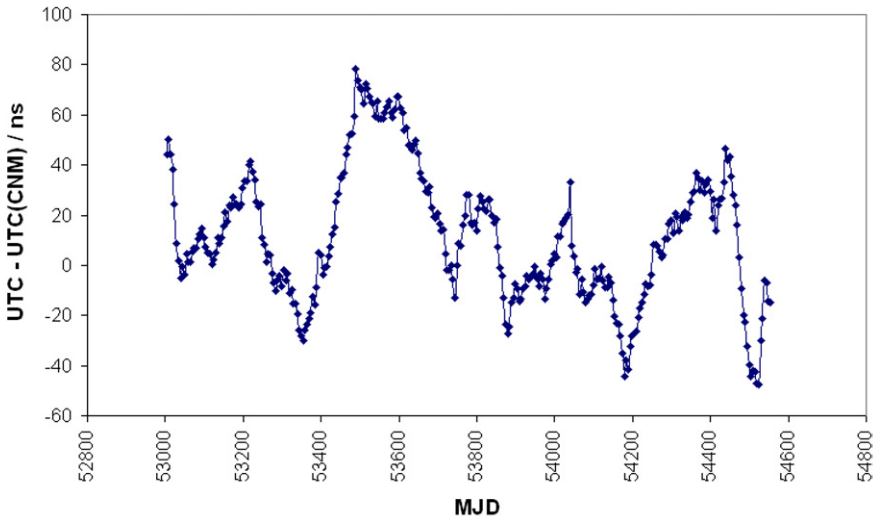

Figure 1. UTC − UTC(CNM) differences as published in the *Circular T* of the BIPM.

preliminary results, and finally, in section 5 we present the conclusions.

2. Algorithm

If a set of N atomic clocks is available, then an atomic time scale TA can be defined in the most simple way as an average of the reading of the clocks by the relation

$$\mathrm{TA}(t) = \frac{1}{N}\sum_{i=1}^{N} h_i(t), \tag{1}$$

where $h_i(t)$ is the reading of the clock i at time t. With this definition of the TA time scale, as can be noted from equation (1), every participating clock has the same weight $1/N$. In this way, every clock in the ensemble has the same level of participation in the generation of the TA. However, in a more realistic scenario it is convenient to take into account that different clocks have different accuracies and frequency stabilities, and so different weights can be assigned to each clock, then the time scale TA can be defined as

$$\mathrm{TA}(t) = \frac{1}{N}\sum_{i=1}^{N} \omega_i h_i(t), \tag{2}$$

where ω_i is the weight of the clock i. Of course, the condition of normalized weights is given by

$$\sum_{i=1}^{N} \omega_i = 1. \tag{3}$$

As a first approach it is possible to define each weight ω_i as constant in time. However, potentially the best scenario is given when a dynamic weighting approach is implemented, which increases or decreases the weight given to a clock according to its frequency stability characteristics, which can change over time for different reasons. In this case the weights can be defined as inversely proportional to the frequency stability of the clock under consideration, where the frequency stability can be measured in terms of the Allan deviation. In this scheme we can define the weights as

$$\omega_i(t) \propto \frac{1}{\sigma_i(\tau)}. \tag{4}$$

Here $\sigma_i(\tau)$ is the Allan deviation of the clock i for an average time τ. The proportional constant is defined by the normalization condition on weights as relation (3). In this way, the TA time scale defined in terms of the dynamic weighting takes the following form:

$$\mathrm{TA}(t) = \frac{\sum_{i=1}^{N}\omega_i(t)h_i(t)}{\sum_{i=1}^{N}\omega_i(t)} = \frac{\sum_{i=1}^{N}\frac{1}{\sigma_i(\tau)}h_i(t)}{\sum_{i=1}^{N}\frac{1}{\sigma_i(\tau)}}. \tag{5}$$

Unfortunately, equation (5) cannot be implemented experimentally as written, because the readings from clocks $h_i(t)$ are not physically observable. Experimentally it is only possible to measure the time difference between pairs of clocks. So, it is possible to rewrite equation (5) in terms of the time differences between participating clocks. By subtracting from each side of equation (5) the reading of clock k at time t we have

$$\mathrm{TA}(t) - h_k(t) = \frac{\sum_{i=1}^{N}\omega_i[h_i(t)-h_k(t)]}{\sum_{i=1}^{N}\omega_i}. \tag{6}$$

If we define $x_k(t)$ as the time difference between clock k and the time scale TA at time t, and define x_{ki} as the difference between clock k and clock i, then equation (6) takes the form

$$x_k(t) = \sum_{i=1}^{N}\omega_i x_{ki}(t), \tag{7}$$

where the normalization condition (3) was taken into consideration. This last equation defines the time scale TA in terms of the time differences $x_{ki}(t)$ among participating clocks.

Because of the condition $x_{ij}(t) = -x_{ji}(t)$, the weighted average of $x_k(t)$ is zero, that is,

$$\sum_{k=1}^{N} \omega_k x_k(t) = \sum_{k=1}^{N} \omega_k \sum_{i=1}^{N} \omega_i x_{ki}(t) = \sum_{k,i=1}^{N} \omega_k \omega_i x_{ki}(t) = 0. \tag{8}$$

Once the time differences $\{x_{ki}(t)\}$ are known, it is then possible to compute the time scale TA by using equation (7). However, it is important to note that this way of computing the time scale TA corresponds to a post-processing scheme. In cases where it is necessary to generate a time scale TA in real time, it is necessary to introduce a scheme of prediction for the time differences of clocks with respect to the time scale TA. One of the simplest models to predict the time difference of a clock with respect to a reference (we assume here that the reference is more stable and accurate than the clock under consideration) is

$$\hat{x}_k(t+\tau) = x_k(t) + \left[y_k(t) + \frac{D_k \tau}{2} \right] \tau + \cdots, \tag{9}$$

where $\hat{x}_k(t+\tau)$ is the prediction of the time difference of clock k with respect to the reference for the future time $t+\tau$. Here $x_k(t)$ is the (known) time difference between clock k and the reference and $y_k(t)$ is the (known) fractional frequency difference at time t. Finally, D_k is a constant accounting for changes in $y_k(t)$ during the time interval $(t, t+\tau)$.

It is opportune to notice that in the case of white frequency modulation (WFM) and random walk frequency modulation (RWFM) the best prediction for the next time interval τ is just given by the average value and by the last time difference value, respectively. In both cases it is easy to show that the mathematical relationship between the prediction uncertainty (prediction error deviation (PED)) and $\sigma_y(\tau)$ is given by $\text{PED} = \tau \cdot \sigma_y(\tau)$. So, the way we select the weighting scheme (equation (4)) in our algorithm, as $\propto 1/\sigma$ and not $\propto 1/\sigma^2$, could optimize the stability of the TA time scale in the long term where the RWFM is the dominant noise. Finally, notice that $\hat{x}_k(t+\tau)$ can be seen as an expansion of the function x_k in terms of a Taylor series around the value $x_k(t)$ for the time interval of τ.

Once the time difference $x_k(t)$ is known through equation (7), it is possible to predict the value of the time scale TA for the time $t+\tau$ using equation (9). Here it is important to note, opposite to equation (8), that the weighted average of the predictions $\hat{x}_k(t+\tau)$ is not necessarily zero; that is,

$$\sum_{k=1}^{N} \omega_k \hat{x}_k(t+\tau) \neq 0. \tag{10}$$

Once the (future) time $t+\tau$ is reached, it is possible to measure the time differences among participating clocks, and then it is possible to compute the value of the time scale TA for that time $t+\tau$. Of course, the predicted value of the time scale TA computed at time t for the time $t+\tau$ will not necessarily be equal to the computation of TA at time $t+\tau$. Under this scheme, the time scale prediction for $t+\tau$ can be corrected by the time difference measurements according to the relation

$$x_k(t+\tau) = \sum_{j=1}^{N} \omega_j [\hat{x}_j(t+\tau) - x_{jk}(t+\tau)]. \tag{11}$$

The prediction $\hat{y}_i(t+\tau)$ of the fractional frequency deviation of clock i with respect to the time scale TA for time $t+\tau$ is made according to

$$\hat{y}_k(t+\tau) = \frac{\hat{x}_k(t+\tau) - x_k(t)}{\tau}. \tag{12}$$

Once the (future) time $t+\tau$ is reached, the correction for the frequency prediction can be made through an exponential filtering defined by

$$y_i(t+\tau) = \frac{1}{1+m_i}[\hat{y}_i(t+\tau) + m_i(\tau) y_i(t)], \tag{13}$$

where m_i is given by

$$m_i(\tau) = \frac{1}{2}\left[\sqrt{\frac{1}{3} + \frac{4}{3}\frac{\tau_{\min,i}^2}{\tau^2}} - 1 \right], \tag{14}$$

and $\tau_{\min,i}$ is the integration time at which the noise floor of clock i is reached.

3. Results

The algorithm presented in the previous section has been implemented at the CENAM Time and Frequency Division on four industrial Cs clocks and one active hydrogen maser. The Cs clocks are identified as CsG, CsH, CsI, CsJ. Clocks CsG and CsJ are standard performance, while CsH and CsI are high performance clocks. According to the manufacturer, frequency stability specifications for Cs clocks for $1\ \text{s} \leqslant \tau \leqslant 10^6\ \text{s}$ are $\sigma_y(\tau) = 5.6 \times 10^{-11}/\sqrt{\tau}$ and $\sigma_y(\tau) = 1 \times 10^{-11}/\sqrt{\tau}$ for standard and high performance, respectively, while for the active hydrogen maser with autotuning cavity the frequency stability specifications are $\sigma_y(\tau) = 1 \times 10^{-12}/\tau^{3/4}$ for $1\ \text{s} \leqslant \tau < 10^2\ \text{s}$ and $\sigma_y(\tau) = 3 \times 10^{-14}/\tau^{1/3}$ for $10^2\ \text{s} \leqslant \tau \leqslant 10^5\ \text{s}$. These specifications for clocks are in good agreement with measurement results discussed in section 4. The time scale TA is computed every hour with the dynamic weighting procedure described in equation (4). A non-commercial system is used to measure the time differences among clocks, which is also referred to as a phase comparator, based on the dual mixer frequency technique, and has a resolution of 20 ps. The phase comparator has 32 input channels, which allows it to compare with that same number of clocks. It performs one time difference measurement every second for each of the 32 channels in use. One Cs clock of the ensemble is selected as the master clock, and all of the other clocks are compared with respect to the master. The results during the implementation of the TA time scale algorithm were obtained from 14 weeks of continuous time scale generation. The following results are considered as preliminary because it is necessary to measure the performance of the time scale TA for a longer period to obtain more confidence in the results. Figure 2 presents a schematic of the time difference measurement system (phase comparator). The clocks are compared through their 5 MHz output signals. The phase comparator measures the time differences among clocks modulo one signal period (200 ns). An acquisition data system, coupled to the phase comparator,

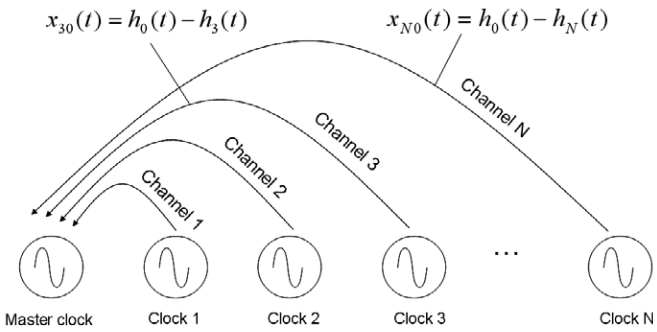

$$x_{ij}(t) = h_j(t) - h_i(t) = [h_0(t) - h_i(t)] - [h_0(t) - h_j(t)]$$

Figure 2. Schematic of the time difference measurement system used at CENAM, also referred to as a phase comparator. The system performs one measurement every second.

processes in real time the phase comparator measurements to obtain the total phase difference $x_{ij}(t)$.

To transform the time scale TA from a virtual time scale (with no 1 pps physical signal defining the time scale) to a real time scale (with a 1 pps physical signal defining the time scale) we use a micro-phase and frequency stepper (MPS). The MPS steers the 5 MHz frequency signal of the active hydrogen maser of the ensemble so that it follows the virtual TA time scale. The output of the MPS is used as another clock of the ensemble in order to measure the time difference between the (virtual) time scale and the corrected frequency of the hydrogen maser. The MPS is controlled by an automatic servo loop so that the time difference between the TA and the MPS output remains constant (figure 3). The weight of the corrected hydrogen maser frequency is exactly zero all the time in order to avoid any self-perturbing loop. Figure 4 shows the phase comparator measurements among clocks from MJD 54 610 to MJD 54 648. The vertical axis corresponds to the time difference of participating clocks with respect to CsI, the master clock. Figure 5 shows the time differences of the participating clocks with respect to the time scale TA from MJD 54 610 to MJD 54 645. As in figure 4, a constant time offset has been applied in order to better appreciate the clocks' performance. Finally, in figure 6 is shown the frequency stability of clocks with respect to the master clock (CsI) and with respect to the TA time scale. The frequency stability of the UTC(CNM) computed from the BIPM *Circular T* for data shown in figure 1 is also shown. The lower solid line corresponds to the estimated frequency stability of the TA time scale. In the next section we discuss the estimation of the TA time scale frequency stability.

4. Discussion

Here we first present a discussion of the results obtained when the CsI clock is used as the master clock. Then we will discuss results when the time scale TA is used as reference.

4.1. Measurement results when CsI is used as the master clock

Due to the high frequency stability of the active hydrogen maser in the short term, the relative frequency stability between CsI and the maser can be considered as a measurement of the frequency stability of the master clock CsI, which is about 1×10^{-13} at 1 h. If the CsI clock is compared with another reference more stable than the maser, we will expect no significant change in this number because it is already limited fundamentally by the CsI clock itself as can be seen in figure 6. A similar argument can be applied to the results for frequency stability measurements of clock CsH, because both clocks CsI and CsH have the same manufacturer's specifications for stability and perform similarly when they are measured in the laboratory. According to the manufacturer, CsI and CsH should have a frequency stability around 1.3×10^{-13} for an average time of 1 h (see section 3), which is in close agreement with our results shown in figure 6. According to figure 6, both CsJ and CsG are less stable than CsI and CsH. This was expected, because both of them are low performance clocks. For an integration time around 1 day or longer, the frequency stability of the MPS departs from the maser stability. We consider that it is due to the frequency correction process on the maser frequency made in order to follow the TA time scale. This suggests that the frequency correction we made on the maser frequency through the MPS is probably too tight. Finally, we would like to mention that for the purpose of evaluating the TA time scale performance, the frequency stabilities of clocks CsJ and CsG are interesting enough to be considered further. As can be noted from figure 6, the frequency stability of these two clocks is slightly better than the manufacturer's specification for standard performance Cs clocks. According to specification, the stability of those clocks could be close to 9×10^{-13} at 1 h; however, measurements show a frequency stability around 3.5×10^{-13} at 1 h for both of them. In any case, because of their relatively large instabilities, if these two clocks are compared with respect to a more stable reference than the CsI clock, like the time scale TA, we will expect no significant changes in the frequency stability results. This can be clearly appreciated in figure 6.

4.2. Measurement results when the TA time scale is used as reference

As we discussed in the previous section, when the TA time scale is used as reference, the frequency stability results for CsJ and CsG are similar when those clocks are compared with respect to CsI. The frequency stability for the CsI clock is slightly better than when it is compared with the maser; this difference increases when the average time increases. For an integration time of 1 h, the stability of CsI when it is compared with respect to the maser is about 1×10^{-13}, which is almost the same value when compared with respect to the TA time scale. However, for an integration time of 10^5 s the stability is 1.9×10^{-14} and 1.4×10^{-14} when compared with respect to the maser and TA time scale, respectively. It is important to mention that it is necessary to take into account the correlation between participating clocks and the

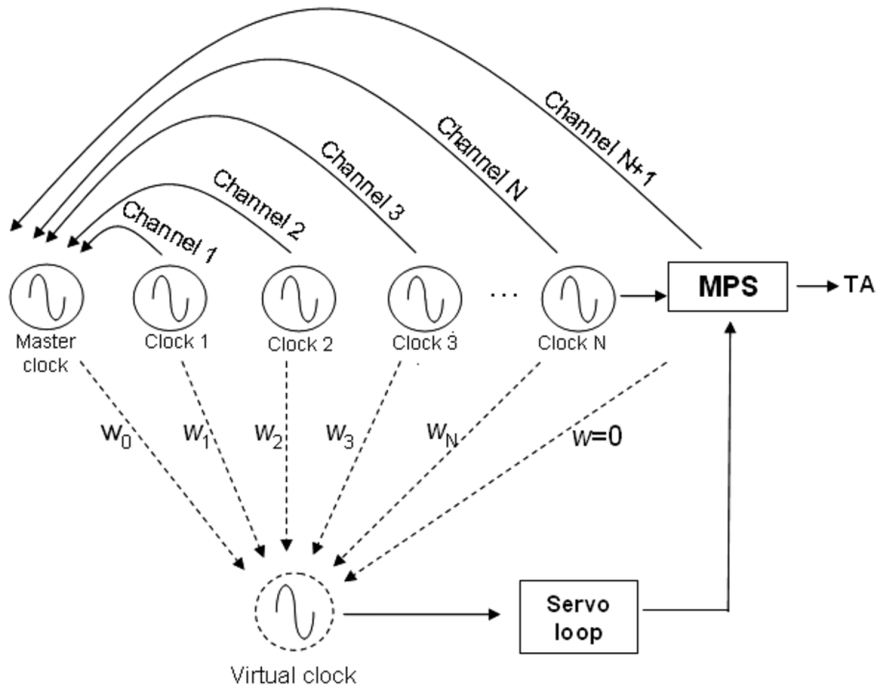

Figure 3. Schematic showing how the output of the micro-phase stepper is held in agreement with the time scale TA.

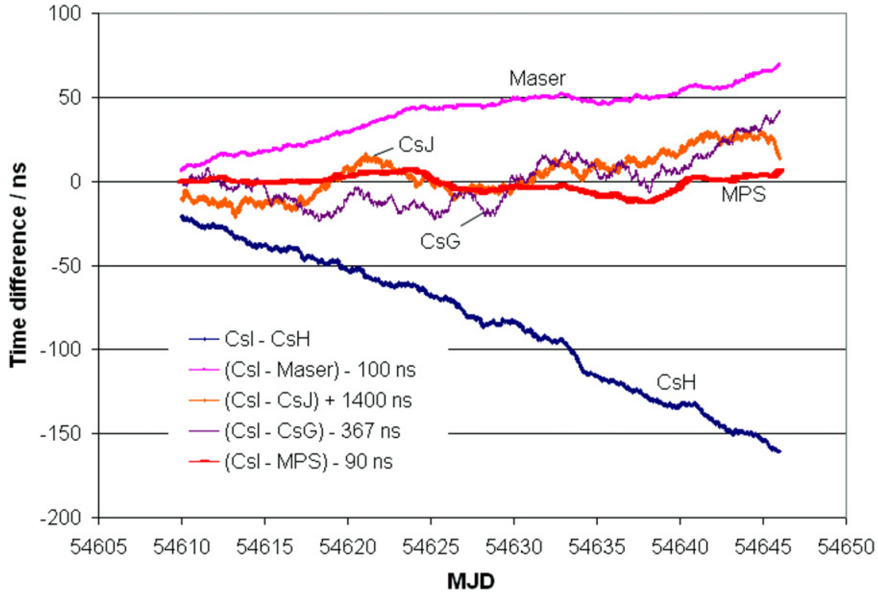

Figure 4. Time difference measurement of participating clocks with respect to the master clock (CsI). The red graph corresponds to the MPS output.

TA scale and then the relative stability is reduced by a factor $1/(1-\omega)$, where ω is the weight of the participating clock. In figure 7 we show the weight for participating clocks on the TA scale for a time period of 30 days. If the correction factor is applied to the stabilities shown in figure 6 and the three cornered hat method is used for $\tau = 10^5$ s for CsI, the maser and TA scale, the stabilities for the maser and TA scale are 9.8×10^{-15} and 8.3×10^{-15}, respectively. The frequency stability difference between the maser and the MPS in figure 6 is due to the corrections of the maser frequency made by the MPS. The MPS corrects the maser frequency once per hour if necessary, causing a small perturbation on the maser frequency stability, as we can see in figure 6. These results suggest that corrections to the maser frequency can be made less often than once per hour, perhaps once per day, and that the magnitude of the corrections can be made smaller. These possibilities will be carefully analysed during the coming months. With the aim of estimating the frequency stability of the TA time scale, the three cornered hat method was applied for frequency stability measurements shown in figure 6 for an average time of 1 h (uncertainty in the Allan deviation is small for that average time). Frequency stability of the TA time scale at 1 h is conservatively near to 5×10^{-14}. This result is in close agreement with measurements obtained with the time and

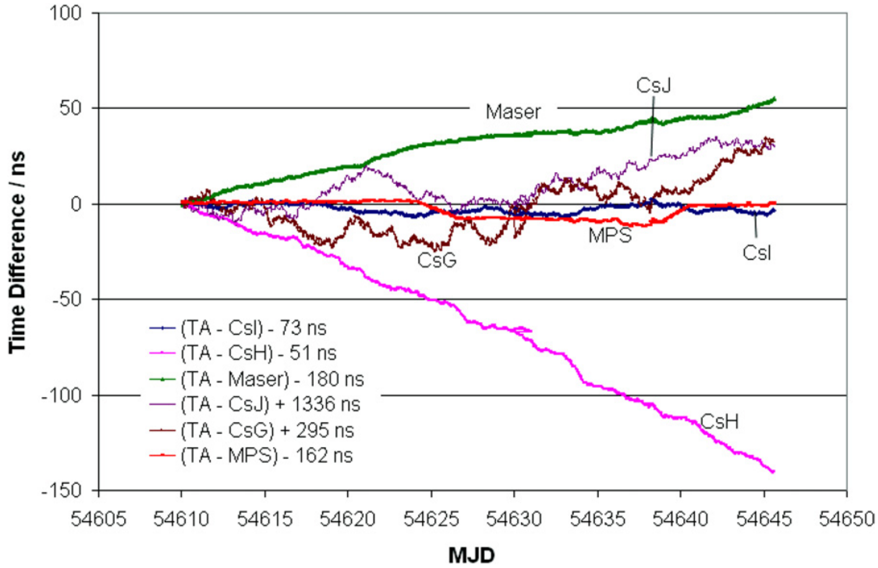

Figure 5. Time difference of participating clocks with respect to the time scale TA.

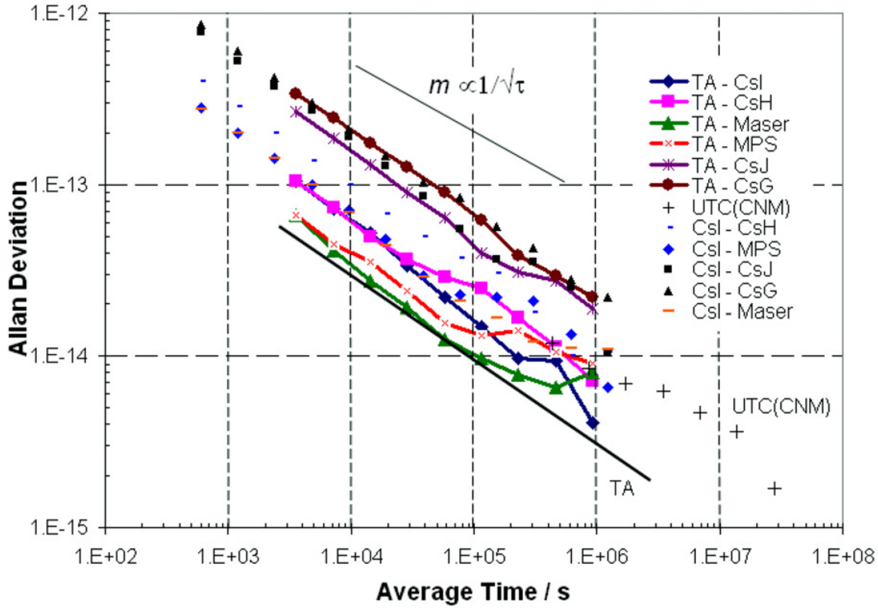

Figure 6. Frequency stability of clocks with respect to the master clock (CsI) and with respect to the TA time scale. The UTC(CNM) stability is also shown according to the BIPM *Circular T* data. The graph corresponding to the best frequency stability is the estimated TA time scale frequency stability.

frequency comparison network of the *Sistema Interamericano de Metrologia* (SIM) [7] when comparing the TA time scale with other SIM time scales, such as UTC(NIST). According to frequency stability results for clocks shown in figure 6, it looks like the TA time scale frequency stability depends on τ as $1/\sqrt{\tau}$. Taking into account the computed value for TA frequency stability at 1 h we can conclude that the frequency stability of TA is nearly described by

$$\sigma_y(\tau) \approx \frac{3 \times 10^{-12}}{\sqrt{\tau}}, \qquad \tau \geqslant 3600\,\text{s}. \qquad (15)$$

This frequency stability is shown graphically in figure 6 as the lower solid line.

5. Conclusions

The CENAM has developed and implemented an algorithm similar to the NIST AT1 algorithm [4] with the aim of improving the UTC(CNM) characteristics of stability, accuracy, availability and robustness. The results of the TA time scale performance are satisfactory. The TA time scale appears to be more stable than any clock participating in its generation. However, the stability of the time scale can probably be improved by optimizing the method used to apply frequency corrections to the maser. The UTC(CNM) time scale will be generated in the near future using the algorithm discussed here. Preliminary results obtained by implementing the TA time scale on four industrial Cs clocks

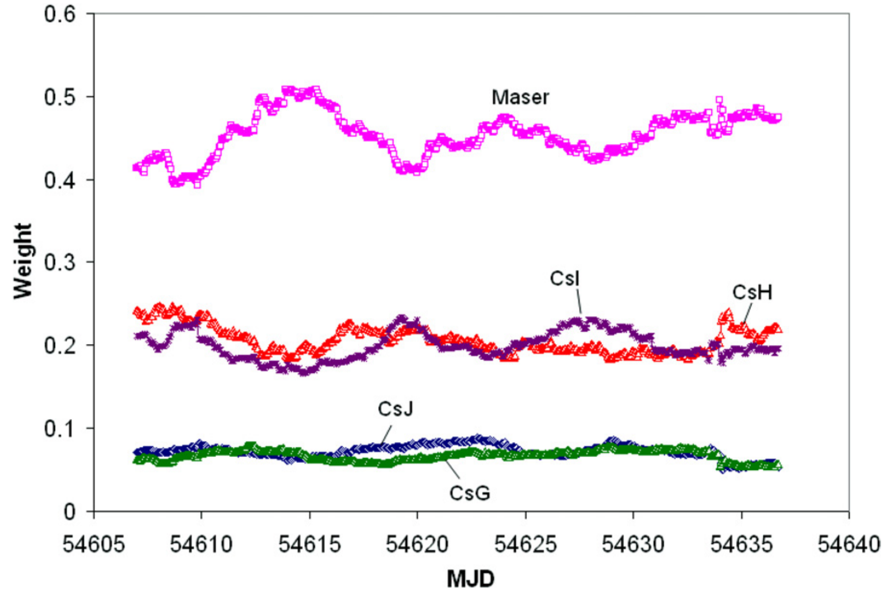

Figure 7. Weight of the participating clocks on the TA time scale for a time period of 30 days.

and one active hydrogen maser are satisfactory and seem to be enough to match the goals for the UTC(CNM) consisting of the |UTC − UTC(CNM)| time difference being no bigger than 25 ns, time stability of 2 ns for 5 days and 15 ns for 1 year. Special care has been taken to implement the algorithm with the robustness required when generating a high performance time scale for critical application. As part of the new scheme of the UTC(CNM) generation, recently a new multichannel GPS receiver has been added to reinforce the comparison of the UTC(CNM) with respect to the GPS time. With those comparison data, according to the BIPM *Circular T*, the UTC − UTC(CNM) uncertainty was reduced from 7.9 ns to 5.6 ns [6]. Last but not least, we would like to mention that the implementation of the TA time scale discussed in this paper is part of the preparation for the SIM time scale generation [7]. The necessary software is currently being added to the SIM time and frequency network that will feed the time scale algorithm with the necessary time difference data. We expect to generate the first preliminary results of the SIM time scale by the end of 2008. Behind the generation of the SIM UTC(k) time scales (excluding the USNO) are about 10 hydrogen masers and 30 Cs clocks; so we are expecting to have a very stable and accurate SIM time scale with the very useful characteristic of being available in almost real time through the SIM time and frequency comparison network [8].

References

[1] BIPM 1996 *Circular T* No 100

[2] Guinot B 1987 Some properties of algorithms for atomic time scales *Metrologia* **24** 195–8

[3] Tavella P and Thomas C 1991 Comparative study of time scale algorithms *Metrologia* **28** 57–63

[4] Weiss M and Weisser T 1991 AT2, a new time scale algorithm: AT1 plus frequency variance *Metrologia* **28** 65–74

[5] Lombardi M A, Novick A N, Lopez J M, Boulanger J S and Pelletier R 2005 The Interamerican Metrology System (SIM) Common-View GPS Comparison Network *Proc. Joint 2005 IEEE Frequency Control Symp. and Precise Time and Time Interval (PTTI) Systems and Applications Meeting (Vancouver, BC, August 2005)* pp 691–8

[6] BIPM 2008 *Circular T* No 245

[7] López-Romero J M, Díaz-Muñoz N and Lombardi M A 2008 Establishment of the SIM Time Scale *Simp. de Metrología (Queretaro, Mexico, October 2008)* submitted

[8] Lopez J M R, Lombardi M A, Novick A N, Boulanger J-S, de Carvalho R, Solis R and Jimenez F 2008 The SIM Network: improved time coordination for North, Central, and South America *European Frequency and Time Forum (EFTF) (Toulouse, France, 23–25 April)*